Alternative Structures for Alternating Poly(dA-dT) Tracts: The Structure of the B-DNA Decamer C-G-A-T-A-T-A-T-C-G†

Hanna Yuan, Jordi Quintana, and Richard E. Dickerson*

Molecular Biology Institute, Department of Chemistry and Biochemistry, and Institute of Geophysics and Planetary Physics, University of California at Los Angeles, Los Angeles, California 90024

Received February 24, 1992; Revised Manuscript Received May 20, 1992

ABSTRACT: The X-ray crystal structure of the decamer C-G-A-T-A-T-A-T-C-G has been solved with two contrasting cations, Ca^{2+} and Mg^{2+}. Crystals with calcium are space group $P2_12_12_1$, cell dimensions a = 38.76 Å, b = 40.06 Å, and c = 33.73 Å, and diffract to 1.7-Å resolution. Crystals with magnesium have the same space group, cell dimensions a = 38.69 Å, b = 39.56 Å, and c = 33.64 Å, and diffract to 2.0 Å. Their structures were solved independently by molecular replacement, beginning with idealized Arnott B-DNA geometry. The calcium structure refined to R = 17.8% for the 3683 reflections greater than 2σ, with 404 DNA atoms, 95 solvent peaks, and 1 $Ca(H_2O)_7^{2+}$ ion. The magnesium structure refined to R = 16.5% for the 1852 reflections greater than 2σ, with 404 DNA atoms, 62 solvent peaks, and 1 $Mg(H_2O)_6^{2+}$ ion. The two structures are virtually identical and are isostructural with C-G-A-T-C-G-A-T-C-G [Grzeskowiak et al. (1991) *J. Biol. Chem. 266,* 8861–8883] and C-G-A-T-T-A-A-T-C-G [Quintana et al. (1992) *J. Mol. Biol. 225,* 375–395]. Comparison of C-G-A-T-A-T-A-T-C-G with C-G-C-A-T-A-T-A-T-G-C-G [Yoon et al. (1988) *Proc. Natl. Acad. Sci. U.S.A. 85,* 6332–6336] shows that the expected alternation of twist angles is found in the central A-T-A-T-A-T region of the decamer (A-T small, T-A large), but the minor groove remains wide at the center, rather than narrow. Minor groove narrowing is produced, in these two structures, not by overwinding of the helix, but by an increase in base pair propeller. This analysis confirms the concept that poly(dA-dT)·poly(dA-dT) is polymorphous, with different local conformations possible in different local environments.

DNA polymers and oligomers containing A·T base pairs have received intense study in recent years. The homopolymer poly(dA)·poly(dT) is known to differ from classical B-DNA, and many different experimental methods have suggested that both a bend in helix axis and stiffness are associated with such "A-tract DNA": slow migration in polyacrylamide gel electrophoresis (Hagerman, 1986; Zinkel & Crothers, 1987), formation of especially small circles by enzymatic ligation (Ulanovsky et al., 1986), and inability to wind around nucleosome cores during reconstitution experiments (Kunkel & Martinson, 1981; Prunell, 1982). In contrast, the alternating heteropolymer poly(dA-dT)·poly(dA-dT) is more like normal B-DNA and is capable of winding around nucleosome cores. Klug et al. (1979) suggested an "alternating B" structure for the AT heteropolymer, with a small helix twist at A-T steps and a large twist at T-A steps. Sequence-dependent differences between the AT homopolymer and heteropolymer may have functional significance in controlling gene expression, including initiation of DNA replication or transcription, and phasing of nucleosome winding.

X-ray crystal structures have been determined for several DNA dodecamers with AT tracts at their centers: C-G-C-G-A-A-T-T-C-G-C-G (Wing et al., 1980; Dickerson & Drew, 1981), C-G-C-G-A-A-T-T-^{br}C-G-C-G (Fratini et al., 1982), C-G-C-A-A-A-A-A-A-G-C-G (Nelson et al., 1987), C-G-C-A-A-A-T-T-T-G-C-G (Coll et al., 1987), C-G-C-A-T-A-T-A-T-G-C-G (Yoon et al., 1988), and C-G-C-A-A-A-A-A-T-G-C-G (DiGabriele et al., 1989). All of these dodecamer structures are isomorphous, with identical crystal packing in the same $P2_12_12_1$ space group. All show a pronounced narrowing of the minor groove in the central AT region and have a bend in the helix axis at the junction of the AT center with the first CG region. It has been suggested (Nelson et al., 1987; Coll et al., 1987) that stiffness may be imparted to the AT homopolymer by cross-strand hydrogen bonds in the major groove between an adenine N6 amine and a thymine O4, on opposite chains of the helix and adjacent base pairs. Such bonds are impossible if A and T alternate along the chain.

Crystal structures have recently been reported from this laboratory for DNA decamers of sequence C-G-A-T-C-G-A-T-C-G (Grzeskowiak et al., 1991; hereafter termed the KK helix) and C-G-A-T-T-A-A-T-C-G (Quintana et al., 1992; hereafter called the TA helix). Although these utilize the same orthorhombic $P2_12_12_1$ space group as the dodecamers, they are not isomorphous with them, packing in quite a different manner. Whereas the dodecamers overlap ends of helices in zigzag columns, the decamers stack end-for-end to simulate continuous helices running through the crystal parallel to the c axis. This orderly packing leads to enhanced resolution, typically 1.3–1.4 Å rather than the 1.9–2.6 Å of the dodecamers.

The TA sequence was planned as a systematic variant of the KK sequence, substituting pyrimidines and purines individually at the center, T for C, and A for G. The result was a mixed-type AT region, A-T-T-A-A-T. In this paper we report the structure analysis of another variant in which the central two bases have been inverted to yield a short alternating tract, C-G-A-T-A-T-A-T-C-G (hereafter termed the AT helix). The new AT structure is isomorphous with KK and TA helices. It offers the opportunity to study different sequences in the same crystal environment and also the same

† Supported by NSF Grant DMB-916261 and NIH Program Project Grant GM-31299.

* Author to whom correspondence should be addressed [phone (310) 825-5864; fax (310) 825-0982].

0006-2960/92/0431-8009$03.00/0

A-T-A-T-A-T sequence in two local sequence and crystal environments: the percent AT decamer and the Yoon et al. (1988) dodecamer.

METHODS

The C-G-A-T-A-T-A-T-C-G decamer was synthesized by the solid-phase phosphoramidite method. Crystals can be grown under high-salt or low-salt conditions and with a choice of cation. Low-salt crystals with magnesium cations were grown by vapor diffusion at 4 °C in sitting drops containing 0.33 mM decamer double helix, 15 mM magnesium acetate, 0.34 mM spermine hydrochloride (pH 6.9), and 10% (v/v) 2-methyl-2,4-pentanediol (MPD). The external reservoir was begun at 15% MPD and was increased 3% per week. Thin plates appeared at 35% MPD. The space group is $P2_12_12_1$, with cell dimensions a = 38.69 Å, b = 39.56 Å, and c = 33.64 Å. Because the thin plates were small (ca. 0.3 × 0.1 × 0.05 mm) and diffracted only to 2.6-Å resolution, they were washed in a solution containing 3 mM magnesium acetate and 30% MPD to remove any surface impurities and then transferred to a DNA solution 25% in MPD but otherwise identical to that from which they grew. These transferred seed crystals then grew to ca. 0.4 × 0.3 × 0.05 mm and gave a diffraction pattern extending out to 2.0-Å resolution.

High-salt crystals with calcium as the cation were grown in a similar manner at 4 °C from a solution containing 0.33 mM double-helical decamer, 140 mM calcium acetate, 0.66 mM spermine hydrochloride (pH 6.9), and 10% (v/v) MPD. The initial reservoir content of 15% MPD was increased 5% per week, and rodlike crystals appeared at 45% MPD. The space group again is $P2_12_12_1$, with cell dimensions a = 35.35 Å, b = 38.46 Å, and c = 33.36 Å. These first crystals were small (ca. 0.3 × 0.1 × 0.1 mm), were usually accompanied by precipitate, diffracted only to 3.0-Å resolution, and were unstable both in solution and in the X-ray beam. With time, single crystals in the sitting drop aggregated into clumps without increasing in size. When water was added to the drop, the aggregated crystals dissolved but the precipitate remained. Re-equilibration of the sitting drop yielded larger and more stable crystals, ca. 0.7 × 0.7 × 0.2 mm. These had cell dimensions a = 38.76 Å, b = 40.06 Å, and c = 33.73 Å, closer to those observed for the magnesium-containing crystals and to the earlier KK and TA decamer helices (Grzeskowiak et al., 1991; Quintana et al., 1992). They diffracted to 1.7-Å resolution.

For ease of reference, the C-G-A-T-A-T-A-T-C-G crystals grown from magnesium acetate will be termed the ATMg crystals, and those from calcium acetate will be called ATCa. For both ATMg and ATCa crystals, X-ray diffraction data were collected at 0 °C on a Rigaku AFC5R diffractometer equipped with a graphite monochromator, using Cu Kα radiation from a rotating anode operated at 8.5 kW. Radiation damage was monitored by three repeatedly measured check reflections. Data were corrected for Lorentz and polarization factors, time-dependent radiation damage, and empirical absorption factors. For the ATMg crystal, of 4601 reflections measured between 8.0 and 2.0 Å, the 1852 greater than $2\sigma(F)$ were used in refinement. In the outermost shell of data, between 2.1 and 2.0 Å, 17% of the reflections still were above the 2σ level. For the ATCa crystal, of 6166 reflections between 8.0- and 1.7-Å resolution, 3683 were above 2σ and were used in refinement. In the highest resolution shell, between 1.8 and 1.7 Å, 25% of the reflections still were above 2σ.

The structure of ATMg was solved by molecular replacement, using the MERLOT program library (Fitzgerald, 1988) to position and orient an idealized B-DNA model (Chandrasekaran & Arnott, 1989) in the unit cell according to the known solution for the C-G-A-T-C-G-A-T-C-G or KK helix (Grzeskowiak et al., 1991). The previously solved KK and TA structures were specifically *not* used as starting points, in order that the AT structure be completely unbiased relative to these helices. The positioned ideal B helix was modified by the X-PLOR rigid body refinement program (Brunger et al., 1987, version 1.5), commencing with the entire double helix as one rigid group and gradually subdividing it into, 4, 10, 20, and 40 groups. Ultimately, individual atom positions were refined with 8.0–2.0-Å data. This model then was subjected to Hendrickson–Konnert positional and B-factor refinement (Hendrickson & Konnert, 1980), using the NUCLSQ routine of Westhof et al. (1985).

Table I: Statistics of Data Collection and Refinement

	ATMg	ATCa
cell dimensions		
a (Å)	38.69	38.76
b (Å)	39.56	40.06
c (Å)	33.64	33.73
resolution (Å)	2.0	1.7
no. of refl over $2\sigma(F)$	1852	3683
final R factor (%)	16.5	17.8
no. of DNA atoms	404	404
no. of water molecules	62	95
no. of cation complexes	1	1
stereochemical refinement parameters[a]		
bond distances (Å)		
bases and sugars	0.017 (0.030)	0.019 (0.030)
phosphates	0.018 (0.025)	0.024 (0.025)
angle distances (Å)		
bases and sugars	0.021 (0.030)	0.025 (0.030)
phosphates	0.026 (0.040)	0.031 (0.040)
planarity (Å)	0.010 (0.020)	0.014 (0.020)
chirality (Å^3)	0.086 (0.100)	0.073 (0.100)
torsion contacts (Å)		
single	0.126 (0.200)	0.113 (0.200)
multiple	0.140 (0.200)	0.115 (0.200)
isotropic B factors (Å^2)		
sugar–base bonds	6.4 (10.0)	5.5 (10.0)
sugar–base angles	7.1 (15.0)	6.3 (15.0)
phosphate bonds	9.3 (15.0)	6.8 (15.0)
phosphate H-bond angles	8.0 (15.0)	7.0 (15.0)
structure amplitudes[b]		
real or A term	20.0	19.0
imaginary or B term	−120.0	−60.0

[a] Numbers in the second part on stereochemical parameters are rms deviations from ideal values in the final model, followed in parentheses by target variance used in refinement. [b] The weight applied to a structure amplitude is the greater of either the experimental σ value or the inverse square of $A + B(\sin^2/\lambda^2 - 0.1667)$.

Because the refined structure did not show the expected narrow minor groove in the center of the A-T-A-T-A-T region, an independent re-refinement was carried out, in which starting coordinates for the A-T-A-T-A-T center were taken from the dodecamer C-G-C-A-T-A-T-A-T-G-C-G (Yoon et al., 1988), which *does* have a narrow minor groove. Under X-PLOR rigid body refinement followed by NUCLSQ, the minor groove widened almost immediately at its center and the structure converged to that which had been obtained previously starting from an ideal Arnott geometry. The root mean square (rms) difference between refined Arnott and "Yoon-center" models was 1.06 Å before refinement and 0.45 Å afterward. Hence, the wide minor groove in the center of the AT region of C-G-A-T-A-T-A-T-C-G can be considered as established beyond doubt.

Solvent molecules were located from $(F_o - F_c)$ difference Fourier and $(2F_o - F_c)$ Fourier maps. Peaks were accepted only if they were simultaneously above the 3σ level in the difference map and above the 1σ level of the Fourier map. Peaks were added at any given stage only if they lay within

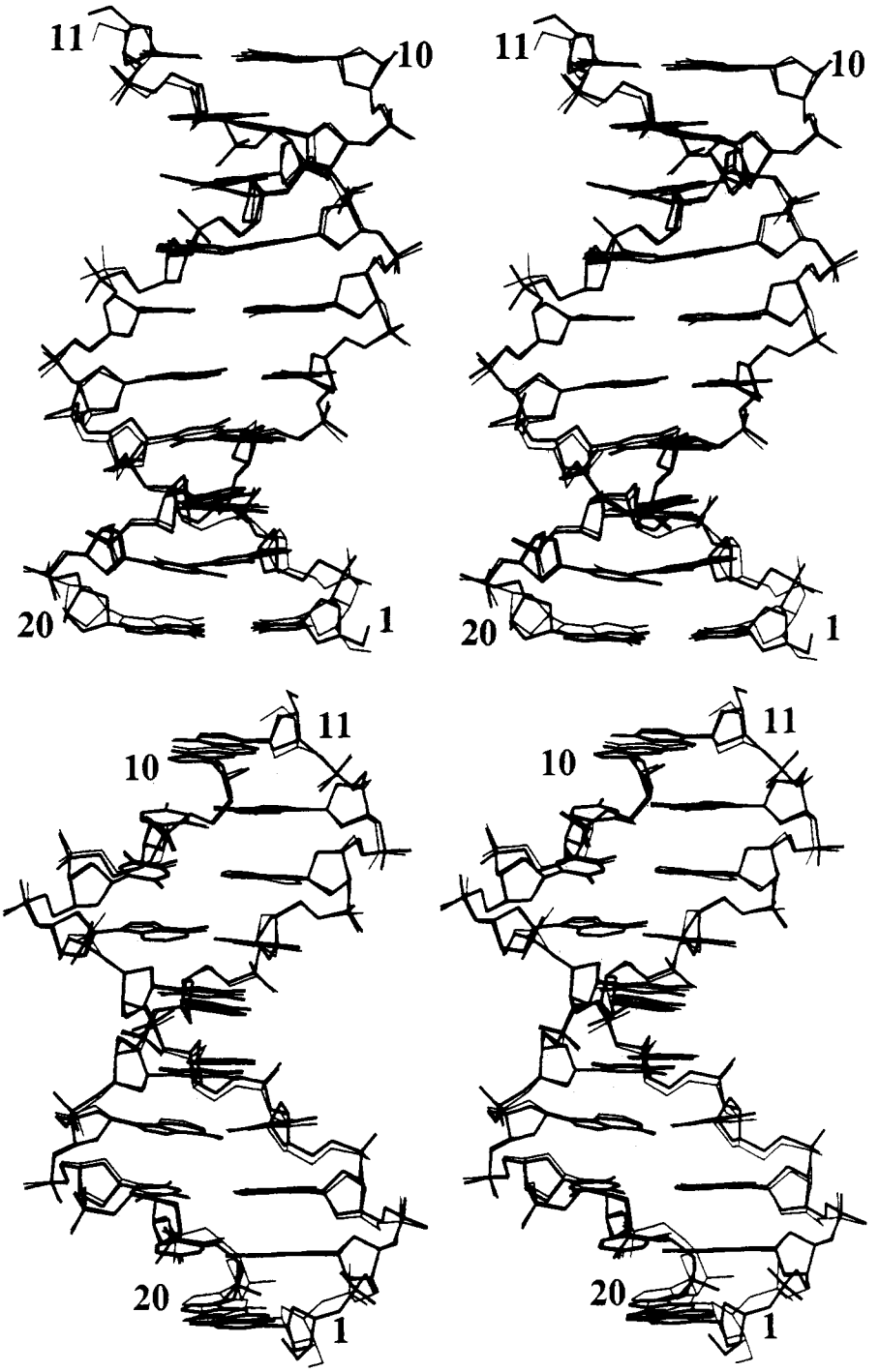

FIGURE 1: Stereo comparison of the two AT decamers, C-G-A-T-A-T-A-T-C-G with Ca^{2+} and with Mg^{2+} viewed (a, top) directly into the center of the minor groove and (b, bottom), 90° to the right, with minor groove above and major groove below. The heavy line is the high-salt ATCa structure with calcium cations, and the light line is the low-salt ATMg structure with magnesium cations. Note that the two structures are essentially identical and that the minor groove is distinctly wider in the center of the A-T-A-T-A-T region (a) than it is to either end of that same region (b).

reasonable hydrogen-bonding distance from DNA atoms or previously assigned solvent molecules. NUCLSQ refinement was continued. The final model at 2.0-Å resolution has 404 DNA atoms, 62 water molecules, and 1 $Mg(H_2O)_6^{2+}$ ion represented by a 7-peak octahedral cluster. The R factor is 16.5% for the 1852 2σ reflections. Refinement statistics are in Table I.

The structure of ATCa was refined independently, again commencing with ideal Arnott geometry. X-PLOR rigid body and segmented rigid body refinement was followed by atomic conjugate gradient refinement, NUCLSQ refinement, and a comparable solvent peak search. The final model at 1.7-Å resolution has 404 DNA atoms, 95 water molecules, and 1 $Ca(H_2O)_7^{2+}$ ion represented by a cluster of 8 peaks. Both the original X-ray intensity data and the final refined coordinates for ATCa and ATMg structures have been deposited with the Brookhaven Protein Data Bank for immediate distribution on request.

RESULTS

Identity of Structure Regardless of Cation or Ionic Strength. The ATMg decamer was crystallized from low salt [15 mM $Mg(OAc)_2$], in contrast to the high-salt conditions of ATCa [140 mM $Ca(OAc)_2$], the TA decamer [140 mM $Mg(OAc)_2$], and the KK helix (300 mM $MgCl_2$). As with KK and TA, survey precession photos of both ATMg and ATCa

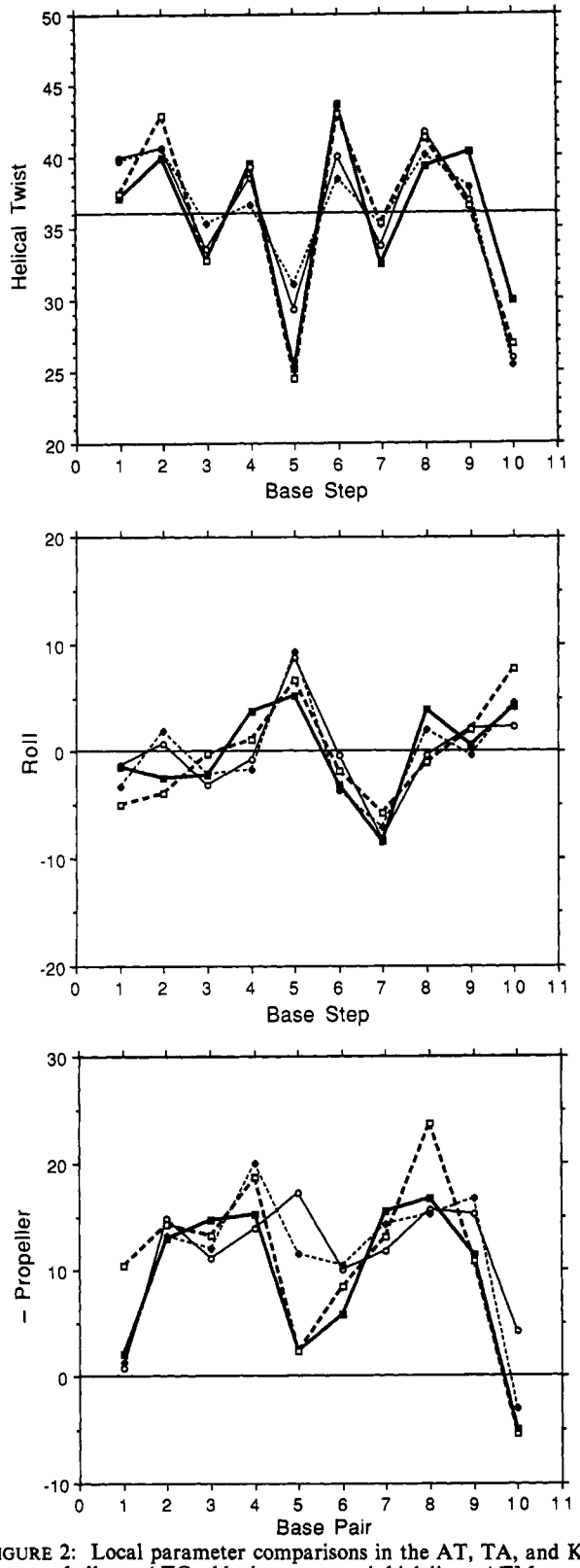

FIGURE 2: Local parameter comparisons in the AT, TA, and KK decamer helices. ATCa, black squares and thick lines; ATMg, open squares and heavy dashed lines; KK, open circles and thin lines; TA, black diamonds and dotted lines. (a, top) Helical twist. The general pattern of alternating twist is the same in all, except that the ATCa twists are slightly more extreme. (b, middle) Roll angles. The AT structure is marginally less extreme than the other two. (c, bottom) Propeller. The AT helix has unusually small propeller in its central two base pairs. (The negative of propeller as defined by the 1988 Cambridge Nomenclature Accords is plotted so that most values are positive.)

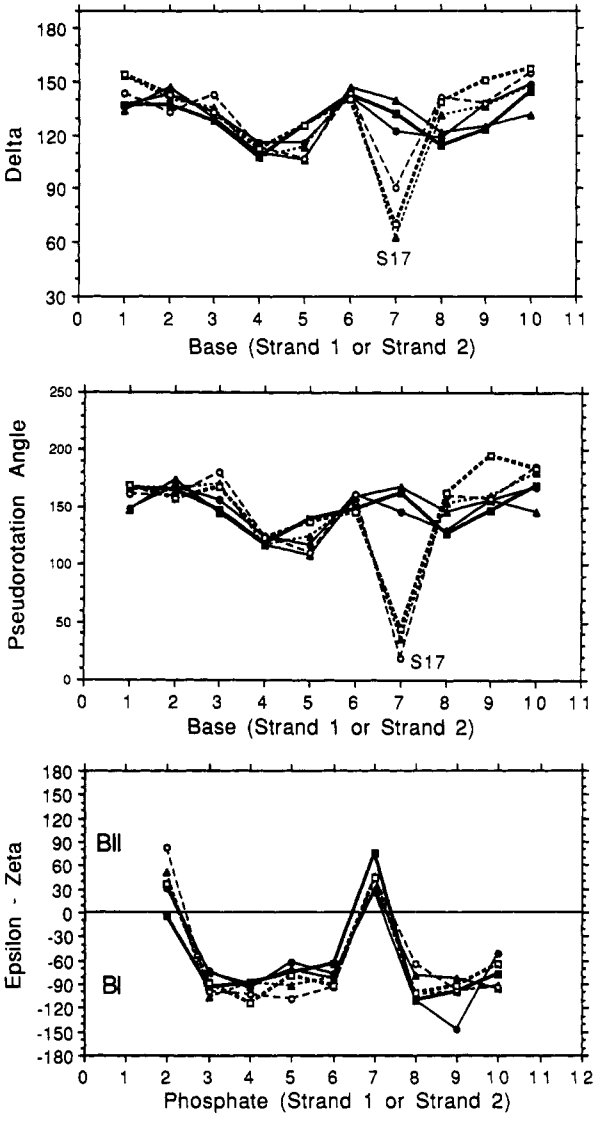

FIGURE 3: Torsion angle comparisons in the AT, TA, and KK decamer helices. ATCa, squares and bold lines; TA; circles; KK, triangles. Strand 1 is denoted by a solid line, whereas strand 2 is dashed. (a, top) Main-chain torsion angles δ (C5′–C4′–C3′–O3′). Note the N conformation of sugar ring S17 in the second strand of all three helices. (b, middle) Pseudorotation angle, again showing the anomalous sugar conformation at S17. (c, bottom) Plot of (ϵ – ζ), showing B_{II} phosphate conformations (positive values) at the second and seventh positions along all six strands.

showed pronounced 3.4-Å streaks that indicate a B-DNA helix aligned along the *c* axis. These streaks were missing from the original ATCa crystals with a shorter *a* axis (35 vs 39 Å) but appeared when those crystals were dissovled and recrystallized. The short-*a* form of ATCa may have its decamer helices inclined at an angle to the *c* axis and interlocking in a manner than allows closer packing in the *a* direction. The structure was not pursued because of the poor degree of order and limited resolution of the crystals (3.0 Å).

The final ATMg and ATCa structures are essentially identical, with a rms difference in atomic positions of only 0.43 Å, most of this difference coming from the terminal sugar–phosphate atoms. Figure 1 shows the two structures superimposed in stereo. The magnesium and calcium cations occupy the same site within the minor groove, although their water coordination geometries differ, as described later. Because of the higher resolution of ATCa than ATMg (1.7 vs 2.0 Å), the remainder of this paper will examine the ATCa structure.

Isostructurality of AT, TA, and KK Helices. The AT, TA, and KK crystal structures are not only *isomorphous* (same space group, unit cell dimensions, and mode of packing within the crystal), they also are *isostructural* (same local helix parameters). Parameters for the ATCa helix are given in

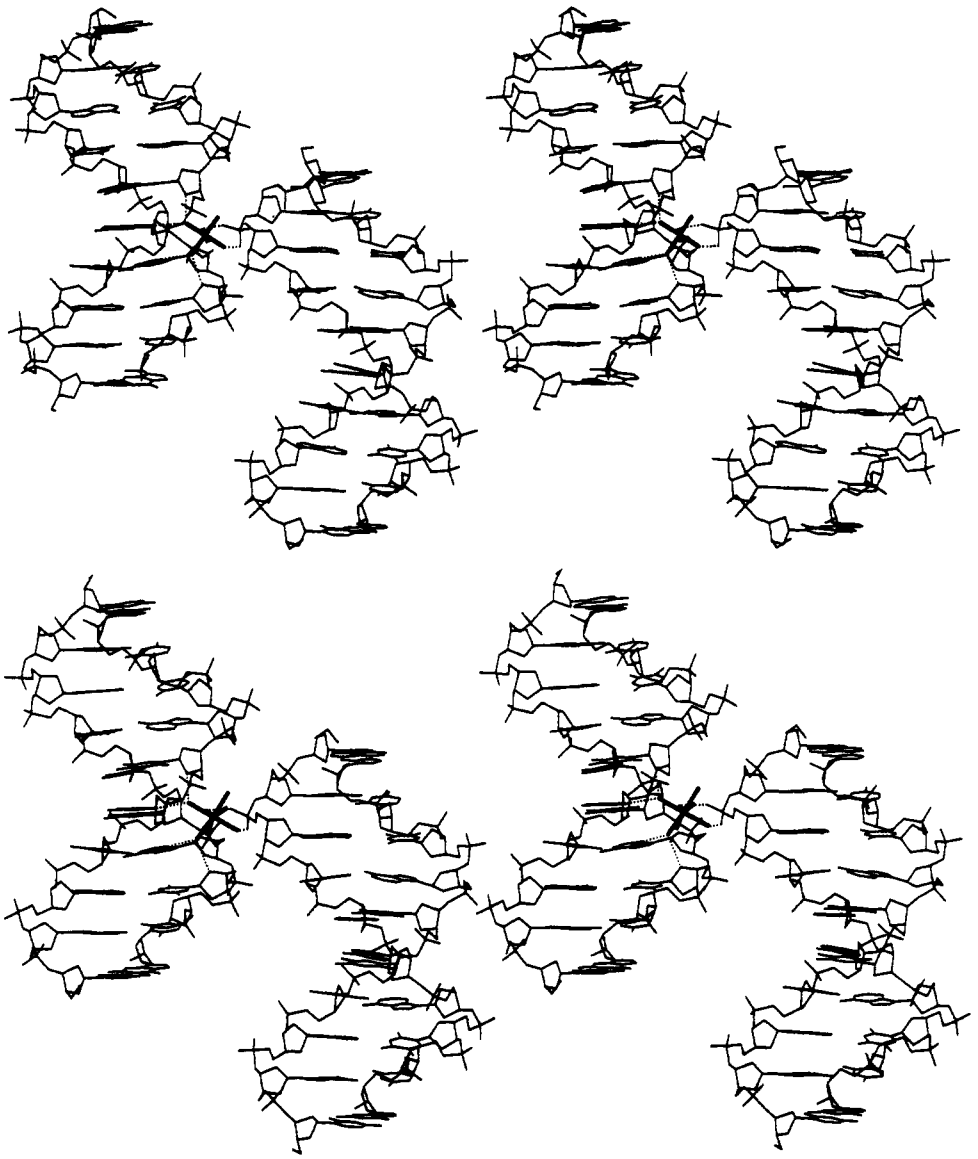

FIGURE 4: Comparison of the interactions of (a, top) $Mg(H_2O)_6^{2+}$ and (b, bottom) $Ca(H_2O)_7^{2+}$ in the ATMg and ATCa decamer crystal structures. In each case the ion sits in the minor groove of one helix, near base pairs T4·A17 and A5·T16, and forms hydrogen bonds to the oxygens of phosphate P3 of a neighboring helix, helping hold the crystal together. See the identical location of a magnesium complex in the TA structure in Figures 7 and 8 of Quintana et al. (1992).

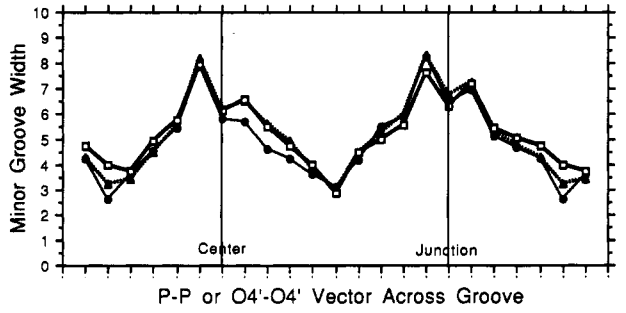

FIGURE 5: Minor groove width in three isomorphous decamer helices in orthorhombic space group $P2_12_12_1$. ATCa, open squares and heavy line; TA, black circles and thin line; KK, black triangles and dotted line. Quantities plotted alternately are shortest distances between sugar O4′ atoms or phosphate P atoms across the groove. O4′–O4′ distances are decreased by 2.8 Å, or two oxygen van der Waals radii. P–P distances are decreased by 5.8 Å, representing two effective phosphate group radii. O4′–O4′ vectors are from oxygen n to oxygen $24 - n$, and P–P vectors are from phosphate n to phosphate $25 - n$. See further identification in Figure 9. The center of the helix and the unbonded junction between two stacked helices are marked.

Table II: Resolution Statistics and Water Comparisons among Four Orthorhombic Decamers and One Related Dodecamer[a]

	helix				
	KK	TA	ATCa	ATMg	Yoon
resolution (Å)	1.5	1.5	1.7	2.0	2.2
refl/base pair	511	379	368	185	160 (1σ)
% refl > 2σ	64	49	66	55	64 (1σ)
waters	142	108	95	62	43
ions	2	1	1	1	0

[a] Intensity data for the Yoon et al. (1988) dodecamer were cut off at the 1σ level rather than 2σ and hence are not directly comparable.

appendix Tables A1–A3, for comparison with equivalent tables for TA and KK helices in Quintana et al. (1992) and Grzeskowiak et al. (1991). The TA and KK helices are inherently more similar, in that their central bases are pyrimidine–purine, whereas this order is reversed in AT. Of the 392 atoms common both to TA and to KK, the root mean square difference in atomic positions is 0.34 Å. In contrast, considering the 366 atoms common to all three decamer helices, the rms difference between ATCa and TA is 0.76 Å and that between ATCa and KK is 0.72 Å.

Twist angles of the three orthorhombic decamer helices are compared in Figure 2a. The pattern of systematic alternation is universal, except that the twist angle excursions from 36° are slightly more extreme in AT than in KK and smallest of

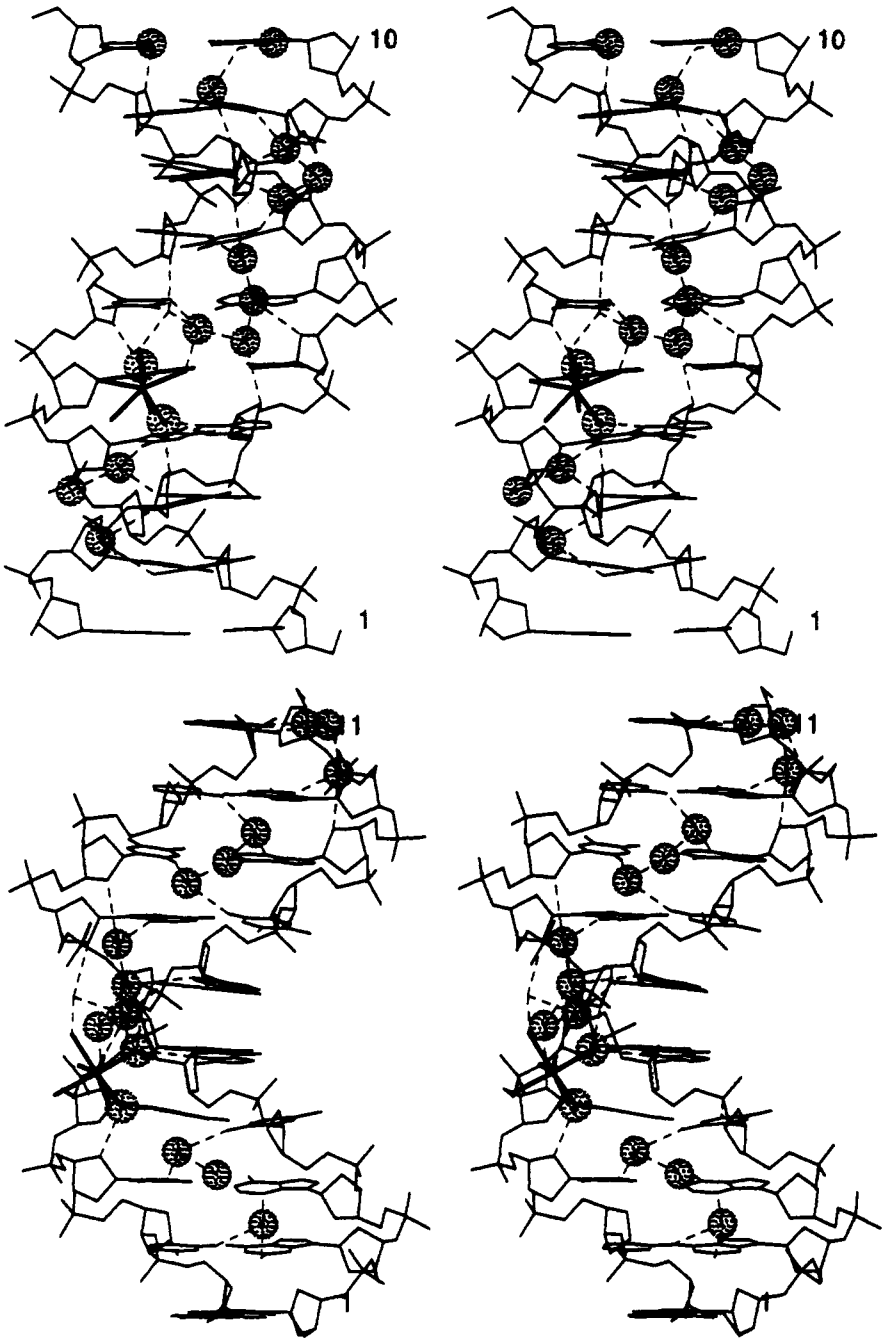

FIGURE 6: Minor groove hydration in the ATCa decamer, viewed as in Figure 1. The double ribbon of hydration in the central wide region of the groove can be seen in (a, top), and the single spine of hydration is visible in narrow regions in (b, bottom). The seven-branched star five base pairs from the bottom of each drawing is the calcium complex.

all in TA. In contrast, roll angles (Figure 2b) are marginally less extreme in AT than in TA and KK. For the TA and KK helices, propeller fluctuates around −15° except for the two outermost base pairs, which are flat (Figure 2c). The AT structure mimics this behavior, except for an unusually small propeller of −5° at the central two base pairs.

Main-chain torsion angles are unremarkable, except for δ (C5′–C4′–C3′–O3′), in which a close crystal contact between helices that affects sugar ring S17 but not the equivalent ring S7 in the other strand is clearly visible for AT, TA, and KK helices (Figure 3a). This deformation, which pushes S17 into an extreme C3′-*endo* or N conformation, is also reflected in pseudorotation angles (Figure 3b). It has been noted earlier in connection with both the TA and KK structures and is clearly visible in Figure 1.

Patterns of phosphate conformation are identical in the three orthorhombic decamers. As Figure 3c shows, phosphates P2 and P7 in one strand and P12 and P17 in the other have a B_{II} conformation, whereas all others are B_I. This confirms a pattern observed earlier with other orthorhombic and monoclinic decamers [see Figure 11 of Grzeskowiak et al. (1991)], by which a local widening of the minor groove is associated with B_{II} phosphate conformations. Other local helix parameters are so similar among the three structures as to be not worth depicting as plots, and the reader is referred to the respective appendix tables.

Bridging of Decamers by Calcium and Magnesium Ions. Intermolecular packing for AT is the same as for TA and KK, as depicted in Figures 1 and 2 of Grzeskowiak et al. (1991) and Figures 4–6 of Quintana et al. (1992). A localized magnesium or calcium ion sits in the minor groove of one helix and makes hydrogen bonds to phosphate oxygens of a neighbor (Figure 4). This contact, the tightest in the entire crystal, produces the deformation in sugar ring S17 that was

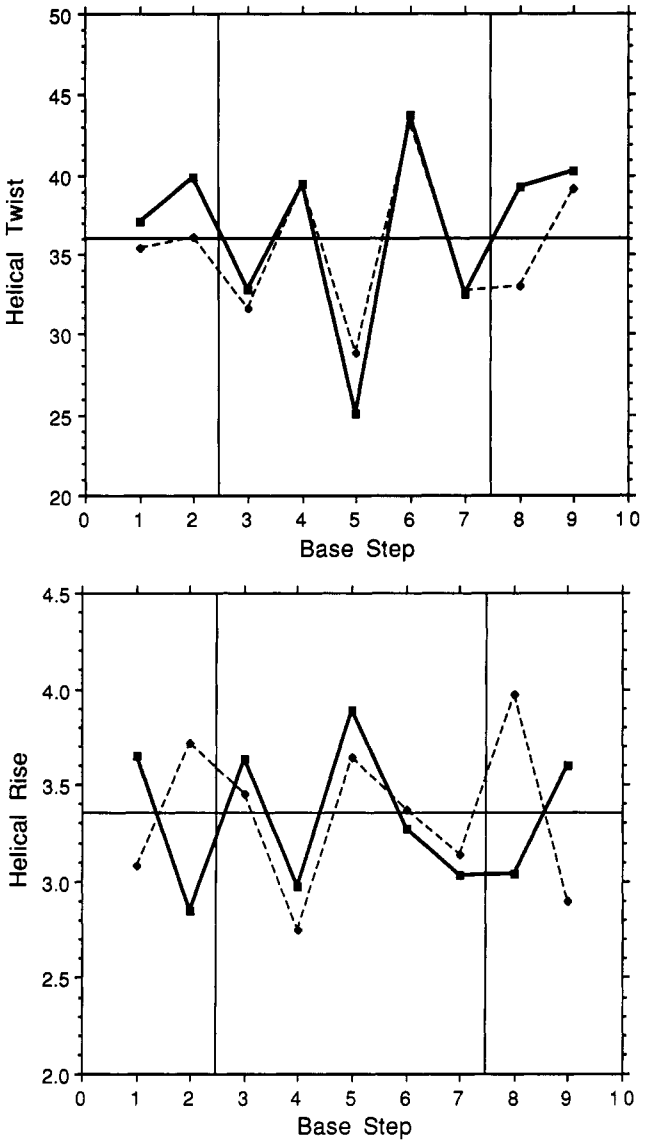

FIGURE 7: Comparison of (a, top) helical twist angles and (b, bottom) base pair rise in this ATCa decamer (solid line) and the Yoon dodecamer, C-G-C-A-T-A-T-A-T-G-C-G (dashed line). Only the central 9 base steps of the 11-step dodecamer are plotted, for comparison with the 9-step decamer. Twist and rise are consistent in the central A-T-A-T-A-T region (steps 3–7) but different elsewhere.

noted in the previous section. For ATMg (Figure 4a), two water molecules of the octahedral complex bond to O1P (3.0 Å) and O2P (3.2 Å) of base A3 of one helix, and two other waters of the complex bond to N3 of A17 (3.2 Å) and N3 of A5 (3.0 Å) of an adjacent helix. The latter bond replaces that to the O2 of base C5 in the KK structure or of base T5 in the TA helix.

In the ATCa structure the calcium ion is heptacoordinated in a pentagonal bipyramid (Figure 4b). Interactions with DNA, however, are virtually the same: two bonds to O1P (3.0 Å) and O2P (2.5 Å) of base A3 in one helix and two others to N3 of A17 (3.0 Å) and N3 of A5 (2.8 Å) in another.

Minor Groove Width and Hydration. Minor groove width in the AT helix matches that seen earlier in TA and KK: wide at the ends of the helix, narrow farther in, but wide once again at the center (Figure 5). The groove width pattern in all three decamers can be represented schematically by C-G-A-T-X-X-A-T-C-G, where the size of type indicates the width of minor groove. For the KK helix with X-X = C-G, this agrees with the earlier generalization based on dodecamer structures: "CG-wide, AT-narrow". But the generalization was contradicted by the TA helix, and it fails again for the present structure. It is not true that A·T base pairs necessarily are associated with a narrow minor groove. But a different generalization remains valid: The minor groove is widest when B_{II} phosphates face one another diagonally across the groove, as P7 and P17 at the center or P2 and P12 across the break between stacked helices. [See Figure 11 of Grzeskowiak et al. (1991).] Furthermore, B_{II} phosphates continue to be associated only with steps where the second base is a purine, A or G, never with Y-Y or R-Y steps.

Fewer water molecules were found in the two AT structures than with KK, which probably is a direct consequence of resolution and of the total amount of experimental data available. Table II compares the nominal resolution and number and percent of reflections per base pair above the 2σ threshold, with the number of ordered water molecules that ultimately could be localized and identified. The critical datum is the number of observed reflections above 2σ per base pair, more than the nominal resolution itself. Although the TA analysis has the same nominal resolution as the KK, it more nearly resembles the ATCa analysis both in quantity of data and in number of waters located. By contrast to TA, the ATMg analysis has half the number of observed data and roughly half as many identifiable waters.

As Figure 6 shows, the ATCa structure exhibits a single minor groove spine of water molecules running down the two narrow regions, and dual ribbons of hydration along the wider regions, as has been observed in all other B-DNA single crystal structure analyses of sufficient resolution. The calcium or magnesium complexes are located at junctions between spine and ribbons, as noted before. No regular pattern of hydration is observed in the major groove, where water molecules make hydrogen bonds with most of the N and O acceptor atoms of base edges.

DISCUSSION

Polymorphism of Alternating AT Oligomers. Runs of exclusively AT base pairs seem to have special behavior patterns in double-helical DNA, patterns that are not encountered in regions of GC or mixed-sequence DNA (Travers & Klug, 1987, 1990; Drew et al., 1990). The alternating heteropolymer, poly(dA-dT)·poly(dA-dT), is known to be more polymorphic and more flexible than either the homopolymer poly(dA)·poly(dT) or heteropolymers involved GC base pairs. Fibers of the alternating AT heteropolymer under suitable conditions can adopt either an A helix or one of the many variants of the B family: B, B′ (narrow minor groove), C, or D (Mahendrasingam et al., 1983). A further and as yet poorly characterized "X-DNA" has been identified for the alternating AT heteropolymer, from circular dichroism studies (Vorlickova et al., 1983). In contrast, fiber diffraction studies indicate that the AT homopolymer is limited to the narrow-minor-groove B′ conformation (Alexeev et al., 1987; Lipanov & Chuprina, 1987). The homopolymer also is more rigid and inflexible than the AT heteropolymer or DNA in general, as measured by its inability to wind around nucleosome cores (Travers & Klug, 1990). GC-containing and mixed-sequence DNA have been observed in A, B (wide minor groove), and Z forms (sequence permitting) but not in the narrow-groove B′.

The polymorphism of alternating AT oligomers probably can be attributed to three factors: (1) the presence of only two hydrogen bonds in an A·T base pair, rather than three as in GC, which allows (but does not necessarily require) the A·T base pair to adopt a higher propeller twist; (2) the systematic inability of alternating AT sequences to form major-groove cross-chain hydrogen bonds, which are believed to

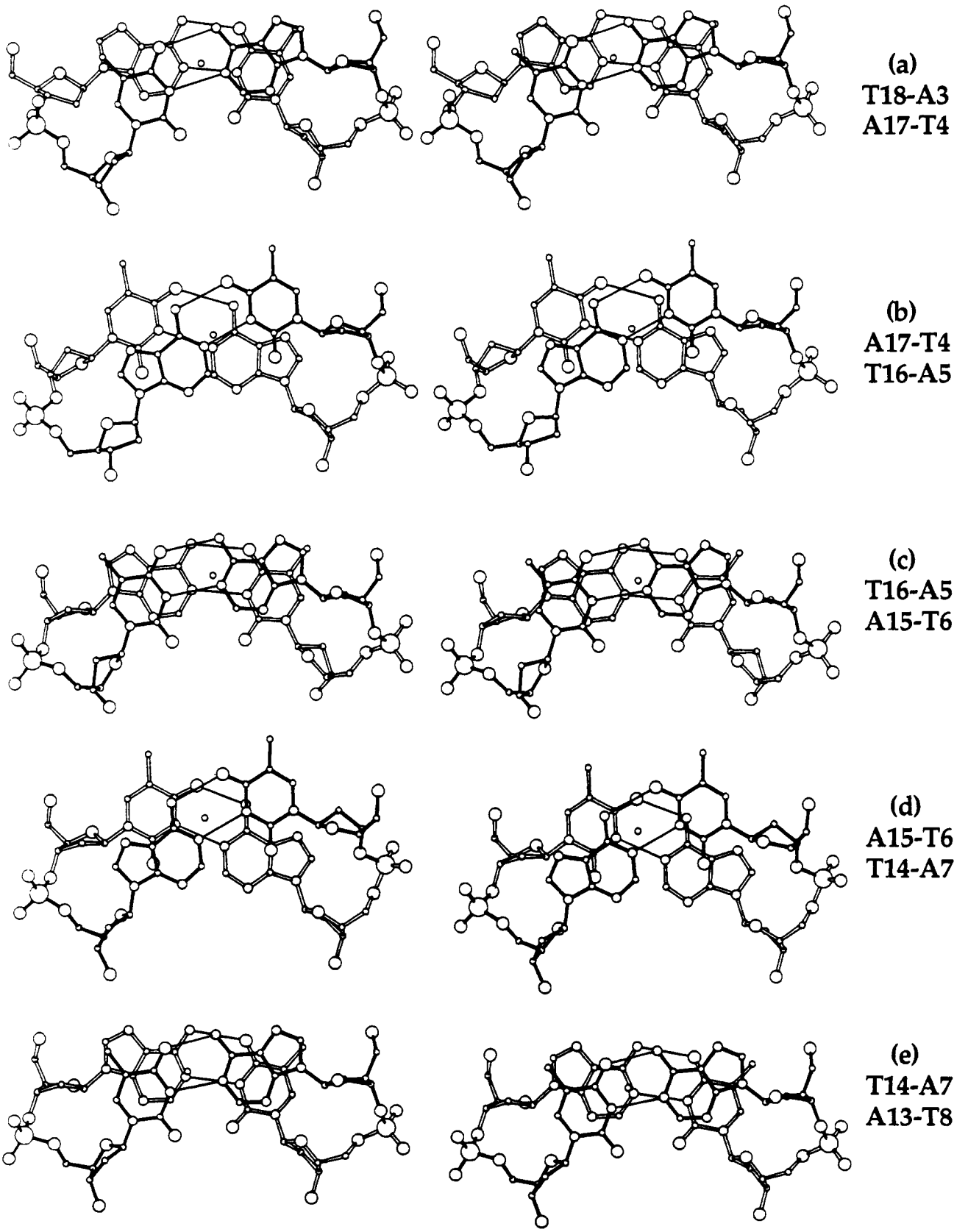

FIGURE 8: Stereoviews of A-T and T-A steps in the ATCa decamer, viewed down the helix axis. Base pair overlap is appreciably greater at the low-twist A-T steps (a, c, e) than at the high-twist T-A steps (b, d). The helix axis (perpendicular to the page) is marked in each stereo by an open dot.

contribute to the rigidity of poly(dA)·poly(dT) regions of double helix; and (3) the inherent instability of stacking at a $^{5'}$T-p-A$^{3'}$ step, which leads to alternations in helical twist.

Examination of Alternating AT Sequence in Two Settings. The alternating AT hexamer, A-T-A-T-A-T, now can be examined in two crystalline double-helical settings: the present C-G-A-T-A-T-A-T-C-G decamer and the dodecamer C-G-C-A-T-A-T-A-T-G-C-G (Yoon et al., 1988). The latter sequence differs from the decamer only in the insertion of C and G three bases in from each end of the helix, but this gives the sequence a regular alternation of purines and pyrimidines, which could induce a different local behavior. Bearing in

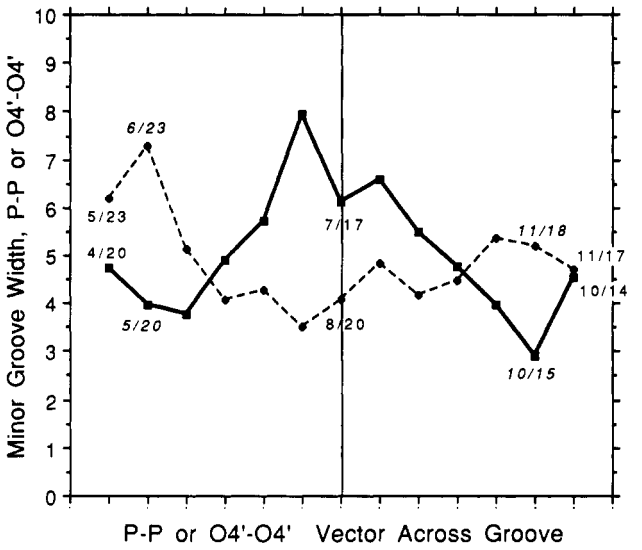

FIGURE 9: Comparison of minor groove width in the AT decamer (solid line) and the Yoon dodecamer (dashed line), both plots being centered on the A-T-A-T-A-T region. Representative O4′–O4′ distances are given in Roman type, as 4/20; representative P–P distances are *italicized*, as *5/20*. See Figure 5 caption.

mind that the lower resolution dodecamer analysis contains less than half as much information per base pair as the decamer (Table II), what can be learned about essential features of poly(dA-dT)·poly(dA-dT) by a comparison of these two crystal structures?

The most striking common feature of the two structures is an identical alternation of twist angles in the central A-T-A-T-A-T region, as seen at steps 3–7 of Figure 7a. This had been expected, of course, ever since the proposal of the alternating B model structure by Klug et al. (1979), but it is reassuring to see this property confirmed yet again. In the explanation proposed in 1979, the intrinsically poor overlap at a T-A step is sacrificed to improve the already good overlap at an A-T step, leading to high twist and low twist, respectively. Precisely this overlap behavior can be seen in views down the helix axis in Figure 8. A consequence of the high twist at T-A steps is that thymine O2 atoms in the minor groove sit squarely over adenine rings in adjacent base pairs, a preference that first was noticed by Heinemann and Alings (1989). Base pair rise is also conserved in the two A-T-A-T-A-T regions, a fact that merely reflects the strong inverse relationship between twist and rise that was noted earlier by Yanagi et al. (1991). Other helix parameters such as buckle and cup show a corresponding alternation at A-T and T-A steps but none so pronounced as twist. In contrast, the behavior of roll seems to be uncorrelated between the two helices.

The most obvious discrepancy between the two structures is the difference in minor groove width behavior, seen in Figure 9. In the dodecamer the AT region is uniformly narrow, whereas in the decamer the groove widens again at the very center of the AT region. Two quite separate but equally interesting questions can be asked about this difference in behavior.

(1) Why is the minor groove width different in these two cases? What factors are responsible for the groove being narrow in the Yoon dodecamer, yet widening in the center of the AT decamer?

(2) Granting the reality of this difference in widths, what helix parameters are altered in order that the change in width be accomplished?

In philosophical terms, we are asking for the *ultimate cause* and the *proximate cause* of the observed structure transformation.

The central six base pairs from the two helices are superimposed in stereo in Figure 10. One point is clear from this and from Figure 7: The proximate cause of groove widening at the center is not a change in twist angles. It has been suggested frequently that a narrowing of the minor groove in B-DNA is produced by overwinding the helix, thus bringing the two walls of the groove nearer one another. While such a mechanistic model could be valid in other circumstances, it clearly is not operative here. In the transition from the AT decamer to the Yoon dodecamer, the center of the minor groove narrows by as much as 3–4 Å, yet helical twist angles are absolutely unchanged. What key helix parameters, then, are altered to accomplish this transition?

Table III shows the linear correlation between minor groove width and the various base pair and base step parameters. For base pairs, minor groove width is measured by smallest P–P distances across the groove, less 5.8 Å. For steps from one base pair to another, groove width is measured by smallest O4′–O4′ distances, less 2.8 Å. These atom or group radii corrections lead to a smooth curve of groove width, as in Figure 9. In both cases, the groove width vector chosen is disposed symmetrically across the base pair or base step, respectively. Among base pair parameters, the most striking correlation is with propeller, for which $R = 0.916$. The groove-narrowing effect of large propeller magnitude was first noted in Figure 9 of Fratini et al. (1982). If overwinding of twist angles is thought of as narrowing the minor groove by bringing the walls of the groove together from left and right, as viewed into the minor groove with helix axis vertical, large propeller has the effect of bringing the walls together from above and below. The connection between propeller and groove width is easily visible for both the present ATCa helix and the Yoon helix in Figure 11.

Several other parameter changes are less strongly correlated with groove width but probably contribute cumulatively to the change in groove geometry. Inclination is negatively correlated, with $R = -0.581$. A negative inclination (counterclockwise rotation of base pairs in the center of Figure 1a) narrows the minor groove by bringing the walls closer from above and below, as does propeller. Among base step parameters the strongest correlation is with tilt ($R = 0.722$), which has the same explanation as inclination. Positive roll (opening the angle between base pairs toward the minor groove), not surprisingly, tends to increase minor groove width. In this particular interhelix comparison, helical twist is totally irrelevant to minor groove geometry, with a correlation coefficient of only $R = 0.055$! Other correlations probably are below the level of significance, in view especially of the low resolution of the C-G-C-A-T-A-T-A-T-G-C-G structure analysis.

Hence we have answered the second of the two questions posed earlier: The *proximate cause* of the widening of the minor groove in the center of the C-G-A-T-A-T-A-T-C-G helix is a flattening of propeller twist in the two central base pairs, supplemented by small cumulative changes in other parameters such as inclination, tilt, and roll. Helical twist has absolutely nothing to do with groove width in this example.

What then is the *ultimate cause* of minor groove widening at the center of the AT decamer helix? The answer most probably is intermolecular packing contacts within this particularly orthorhombic crystal form. Nearest-neighbor interactions in the A-T-A-T-A-T region are quite different between the C-G-C-A-T-A-T-A-T-G-C-G dodecamer and the C-G-A-T-A-T-A-T-C-G decamer, even though they both happen to utilize the same space group, $P2_12_12_1$.

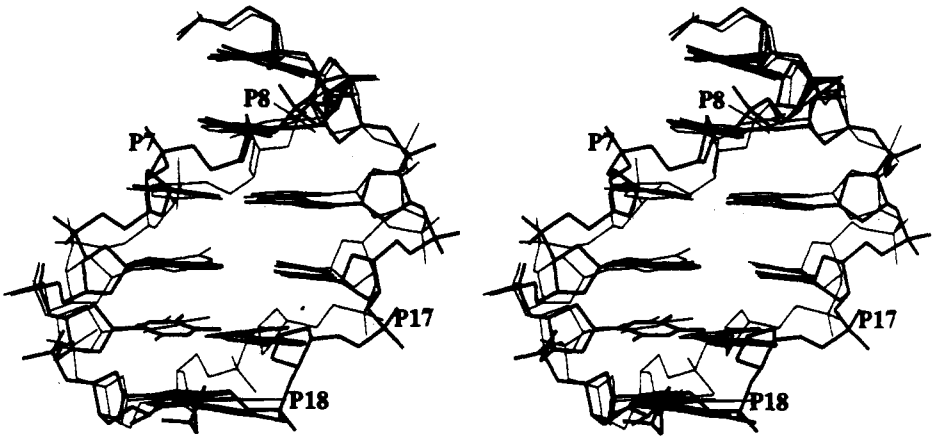

FIGURE 10: Stereoview of least-squares fitting of the central A-T-A-T-A-T regions of this ATCa decamer (heavy line) and the Yoon dodecamer (thin line). Only base pair atoms were used in the fitting. Root mean square differences in atomic position are 0.83 Å for base pair atoms, 1.1 Å for backbone atoms, and 1.01 Å for all atoms.

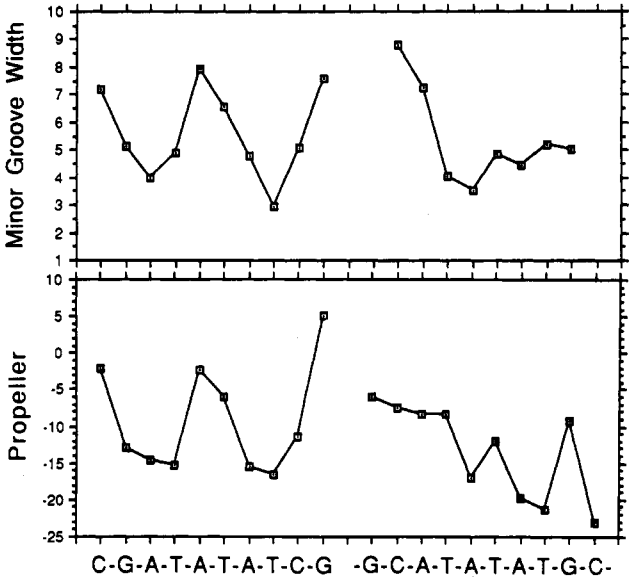

FIGURE 11: Comparison of minor groove width and propeller for the AT decamer (left) and the Yoon dodecamer (right). Only P–P groove width points are plotted, as the P–P vectors are symmetrical across individual base pairs and hence correlate with a given propeller value. (Note that the quantity plotted here is propeller, not its negative, in order that maxima and minima coincide with those of minor groove width).

Table III: Linear Correlation Coefficients between Minor Groove Width and Other Helix Parameters in Yoon and AT Helices[a]

base pairs (P–P distances)		base steps (O4′–O4′ distances)		angles (P–P distances)	
inclination	–0.581	tilt	0.722	α	0.281
tip	0.525	roll	0.603	β	0.385
buckle	0.279	cup	0.000	γ	–0.465
X displacement	0.000			δ	0.591
Y displacement	–0.329	slide	0.569	ϵ	0.678
		twist	0.055	ζ	–0.507
		rise	0.336		
propeller	0.916				

[a] Related base pair and base step parameters are listed on the same horizontal line.

Figure 5 shows that the decamer minor groove is wide both at the center and also at the junctions between two stacked helices. Figure 2 of Grzeskowiak et al. (1991) and Figure 4a of Quintana et al. (1992) illustrate for the identically packed KK and TA helices that the center and the junctions are precisely those regions lying in tight lateral contact with adjacent columns of helices in an *ac* plane through the crystal. The two walls of the minor groove may be opened apart by these contacts: at the center of each helix and at each interhelix junction. In contrast, the minor groove at one-fourth and three-fourths of the way along the helix is packed within the jaws of the major groove of adjacent helical columns in a *bc* plane through the crystal, as illustrated in Figure 1 of Grzeskowiak et al. (1991). Hence, the minor groove probably is narrowed by intermolecular contacts at one-fourth and three-fourths of the way along the helix and widened by different intermolecular contacts at zero, one-half, and one.

By contrast, all of the published dodecamer structures, without exception, appear to have their central minor grooves artificially narrowed by lateral contacts from neighboring helices. Figure 3 of Dickerson et al. (1987) shows especially tight contacts between overlapping ends of neighboring helices and phosphates P7 and P19 flanking the minor groove of a given helix. The effect of these and adjacent close contacts could be to compress the minor groove in the center of the dodecamer, just as the effect of the overlapping of ends may be to open up the minor groove at the two ends of the helix.

Hence, the observed minor groove geometry in both C-G-A-T-A-T-A-T-C-G and C-G-C-A-T-A-T-A-T-G-C-G may be explained ultimately by lateral packing forces within the crystal. This does not mean, however, that crystal packing is the entire story. The only sequences that yet have been observed to crystallize in the dodecamer mode are those with central runs of AT base pairs—either homopolymers such as C-G-C-A-A-A-A-A-A-G-C-G that demand a narrow groove or alternating sequences such as C-G-C-A-T-A-T-A-T-G-C-G that at least tolerate a narrow groove. No dodecamer to date has been induced to crystallize in this form with only GC base pairs throughout. Indeed, the only pure CG decamer solved to data abandons the B form entirely in the crystal and crystallizes as A-DNA (Verdaguer et al., 1991). It may be that GC-containing helices refuse to crystallize in the "Drew" orthorhombic packing mode, simply because their sequences are incompatible with the narrow central minor groove that is required by the crystal packing shown in Figure 3 of Dickerson et al. (1987). Hence, we can say that a given DNA sequence selects those crystal packing modes that impose only deformations with which that sequence is compatible. The crystal itself can be used as a "jig" or template on which to study sequence-dictated helix deformability.

One must avoid the simplistic assumption that propeller and minor groove width are related in an absolute and lock-step fashion. The equation "propeller = minor groove width" is as incomplete as is the once-honored equation "one particular base sequence = one particular helix structure". Many factors interact to determine local helix structure. The strength of

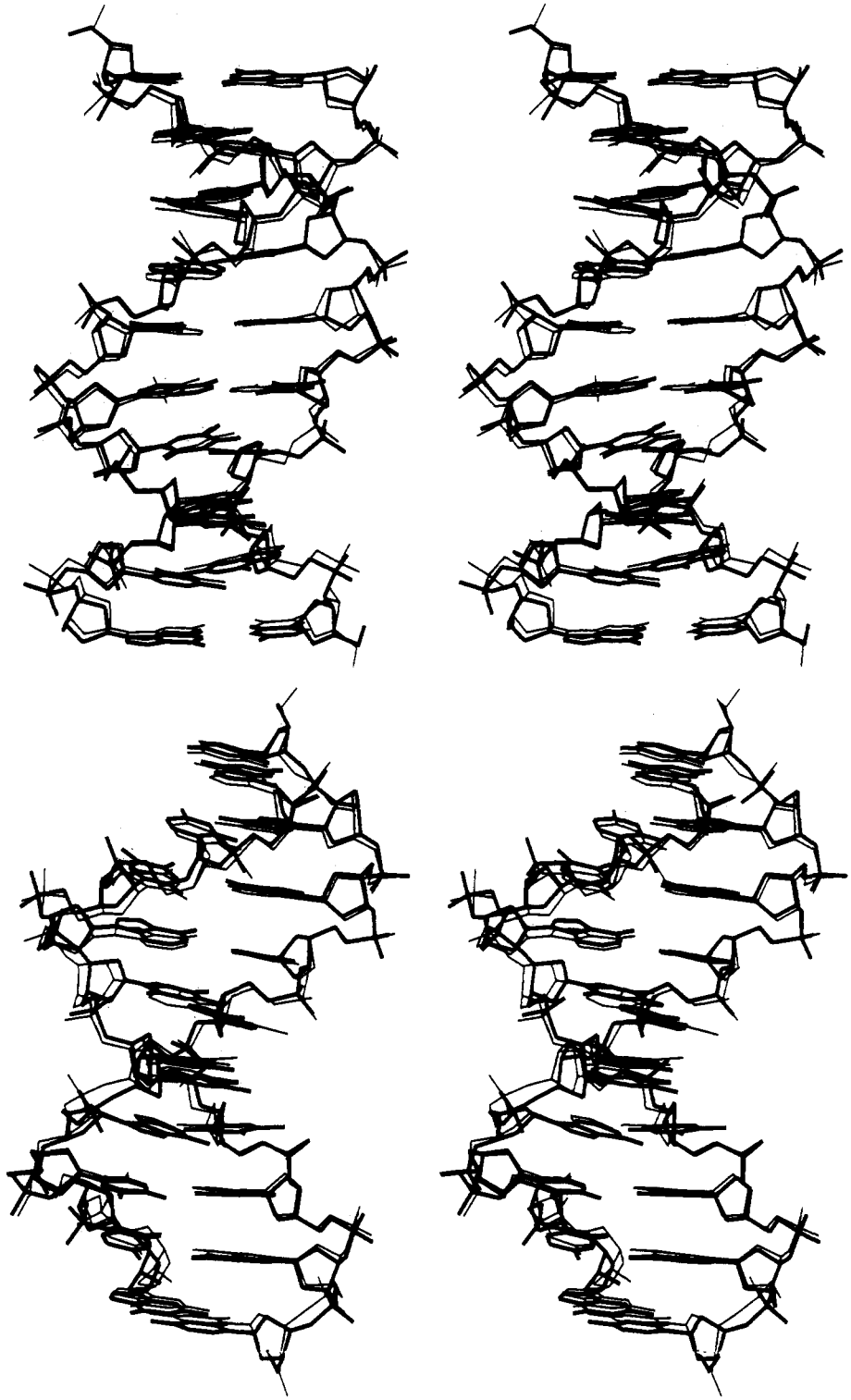

FIGURE 12: Stereoviews of least-squares fitting of the AT helix (dark line) atop the TA helix (light line). (a, top) View into minor groove at center; helix oriented as in Figure 1a. (b, bottom) 90° view tilted to look obliquely along top of central two base pairs. Note that the light-line TA helix backbones are closer to one another across the minor groove in the middle of the helix (a), whereas the light and dark backbones nearly superimpose farther toward the end of the helix (top of b).

the comparison of Yoon and AT helices is that local base sequence differences have been eliminated. "Other things being equal, high propeller leads to narrow groove width". But what if other factors are not equal?

Comparison of the AT and TA helices illustrates the propeller-inducing effect of major groove cross-chain hydrogen bonds. Such bonds, between NH_2 donors and C=O acceptors, were first noticed by Nelson et al. (1987) and Coll et al. (1987) and have been discussed in more detail by Heinemann and Alings (1989) and Yanagi et al. (1991). The latter authors point out that such helix-stabilizing hydrogen bonds are possible only at 4 of the 10 possible base pair steps, C-C (=G-G), C-A (=T-G), A-C (=G-T), and A-A (=T-T), and no others. Hence, two such cross-chain bonds become possible as soon as the central sequence of the decamer is changed from A-T-A-T-A-T to A-T-T-A-A-T. These two new bonds stabilize a larger propeller twist at the center of the AT region in the TA decamer (Figure 2c), but intermolecular contacts persist in keeping the minor groove wide at the center. How can the TA decamer have both a wide central minor groove and large propeller twist in the two central base pairs?

Table A1: Torsion Angles for the ATCa Decamer

	Alpha	Beta	Gamma	Delta	Pseud	Epsil	Zeta	Chi	Ep-Ze
Str.1	---	---	31.8	137.5	166.9	216.7	222.7	244.0	-6.0
	316.4	156.4	37.5	138.3	169.2	168.6	263.2	262.2	-94.6
	295.9	169.7	53.2	128.3	149.1	180.9	273.0	249.2	-92.0
	296.3	171.4	54.7	108.6	118.4	180.4	253.2	246.8	-72.8
	305.5	171.2	51.0	127.1	143.2	197.7	262.8	245.7	-65.1
	300.8	171.9	38.7	142.0	148.1	246.6	170.6	263.1	76.0
	299.0	145.8	39.8	133.3	168.6	171.7	277.2	254.5	-105.5
	302.5	172.9	45.4	113.8	125.8	168.4	269.9	248.9	-101.5
	301.9	173.7	58.8	124.2	148.4	191.1	267.7	246.8	-76.6
	305.5	191.7	23.2	144.9	175.1	---	---	284.5	---
Str.2	---	---	324.9	156.2	173.2	218.3	182.8	270.3	35.5
	304.2	142.7	49.4	143.2	160.3	165.9	257.6	257.3	-91.7
	301.7	196.1	49.2	133.5	174.8	165.8	279.2	261.2	-113.5
	287.6	184.5	63.0	111.2	121.0	180.8	260.2	245.4	-79.4
	304.8	173.5	51.6	127.9	146.4	177.1	266.3	265.1	-89.2
	305.5	176.5	41.9	140.7	146.7	240.4	194.6	266.5	45.9
	283.4	125.2	66.9	72.7	48.2	185.6	284.5	200.6	-99.0
	299.5	176.5	60.9	138.5	161.6	181.0	266.5	239.5	-85.4
	328.9	200.6	3.8	150.0	197.3	175.6	241.7	260.8	-66.0
	31.6	152.8	335.0	160.2	189.7	---	---	281.3	---
AV =	287.3	169.6	74.0	131.6	151.6	189.6	249.6	254.7	-60.1
SD =	64.6	19.2	88.6	19.5	32.2	24.8	34.1	17.7	57.2
DI =	39.1	16.7	73.0	16.0	26.8	9.8	13.7	14.8	17.8

Table A2: Base Step Parameters for the ATCa Decamer

	Roll	Tilt	Cup	Slide	Twist	Rise	Dxyl	Dxy2	Profile
C1-G2	-1.40	1.98	-8.47	0.76	37.1	3.65	3.63	4.00	-8.9
G2-A3	-2.50	-0.70	11.17	-0.18	39.9	2.85	3.89	4.12	22.3
A3-T4	-2.17	-1.74	-10.05	-0.44	32.8	3.63	3.34	3.49	-13.5
T4-A5	3.76	0.12	14.34	-0.16	39.5	2.97	3.96	3.74	17.9
A5-T6	5.25	1.98	-5.99	0.04	25.1	3.89	2.65	2.46	-27.7
T6-A7	-3.04	0.74	-0.90	1.05	43.7	3.27	4.24	3.83	10.6
A7-T8	-8.41	-0.29	-0.55	-0.19	32.5	3.03	3.44	3.83	7.4
T8-C9	3.83	-2.56	10.46	-0.08	39.3	3.04	3.89	4.41	13.6
C9-G10	0.58	-0.26	-7.33	0.92	40.3	3.60	3.43	3.15	-5.5
G10-C1	4.11	0.72	-2.68	0.24	29.9	3.73	2.81	3.19	-17.0
AV =	0.00	0.00	0.00	0.20	36.0	3.37		3.58	
SD =	4.19	1.42	8.65	0.51	5.6	0.36		0.53	
DI =	4.27	2.11	5.32	0.34	1.7	0.23		0.31	

Table A3: Base Pair Parameters for the ATCa Decamer

	Tip	Incl	Prop	Buck	X Dsp	Y Dsp
C1	2.20	-0.27	-2.16	-3.58	-1.09	-1.47
G2	0.80	1.71	-12.98	-12.05	-1.78	0.23
A3	-1.69	1.00	-14.65	-0.87	-1.07	0.96
T4	-3.86	-0.73	-15.21	-10.93	-0.10	0.80
A5	-0.11	-0.61	-2.36	3.41	0.33	0.60
T6	5.14	1.37	-5.90	-2.58	0.46	0.44
A7	2.10	2.11	-15.49	-3.49	0.73	0.96
T8	-6.31	1.81	-16.63	-4.04	1.12	0.07
C9	-2.49	-0.73	-11.41	6.42	0.81	-0.75
G10	-1.91	-1.00	4.94	-0.90	0.76	-0.28
AV =	0.00	0.47	-9.19	0.00	0.02	0.00
SD =	3.30	1.21	7.16	6.22	0.97	0.79
DI =	3.35	1.76	2.89	6.05	1.52	1.22

Careful inspection of superpositions of TA and AT decamers in Figure 12 shows that even here minor groove width depends on propeller magnitude. From Figure 2c, the greatest increase in propeller from AT to TA helices occurs at base pairs 5–16 and 6–15. Rotation of bases 5 and 6 pulls the light-line TA chain downward at the left center of Figure 12a, and rotation of base 16 pulls the other chain upward. As a consequence, this diminishes the distances P8/P17, O8/O16, and P9/P16 in TA, causing its groove width curve to lie lower than that for AT, just to the right of the vertical line marked "Center" in Figure 5. Hence, the most significant difference in groove width plots between AT and TA decamers, as also with the AT vs Yoon comparison, correlated with the most significant difference in propeller magnitude. Changes in helical twist appear not to be involved at all.

Helix Polymorphism and Selection of Preferred Crystal Packing Mode. The orthorhombic decamer crystal form that is adopted by the KK, TA, and AT decamers has special packing requirements, involving a widening of the minor groove at the center of the helix. The A-T-A-T-A-T region of the AT decamer is sufficiently polymorphous to adapt to such a geometry. The A-T-T-A-A-T and A-T-C-G-A-T regions of the TA and KK decamers at least are capable of this geometry; one cannot say without further evidence from the same sequences in other settings that this is the only geometry that they will tolerate. Other sequences such as C-C-A-A-C-G-T-T-G-G, C-C-A-A-G-A-T-T-G-G, and C-C-A-G-G-C-C-T-G-G find the packing constraints of the orthorhombic decamer mode intolerable and select a monoclinic packing instead.

In summary, the A-T-A-T-A-T sequence clearly is polymorphous and capable of adopting more than one configuration depending upon its local environment. The environment in this study has been lateral contacts with other decamers in a crystal, but the same polymorphism should be expressed in contacts with drug molecules and with repressors and other control proteins. Other sequences such as AT homopolymers and sequences with high GC content should be less polymorphous, and one would expect to find them exhibiting a smaller range of conformation. More information is needed about key sequences in more than one crystal setting, especially those with high GC content.

ACKNOWLEDGMENT

We thank Kazunori Yanagi for advice in the early stages of the analysis and for a legacy of useful programs. We also thank Kazimierz Grzeskowiak for advice on DNA synthesis and purification.

APPENDIX: TABLES OF LOCAL HELIX PARAMETERS

Appendix Tables A1–A3 list local helix parameter values along the ATCa helix. Values for the ATMg helix are virtually identical and can be calculated from atomic coordinates using the NEWHEL92 helix analysis program. Both coordinates and program are currently available from the Brookhaven Protein Data Bank. For description and definitions of parameters, see the appendix to Grzeskowiak et al. (1991).

REFERENCES

Alexeev, D. G., Lipanov, A. A., & Skuratovskii, I. Ya. (1987) *Nature 325*, 821–823.

Brunger, A. T., Kuriyan, J., & Karplus, M. (1987) *Science 235*, 458–460.

Chandrasekaran, R., & Arnott, S. (1989) In *Landolt-Bornstein, New Series, Group VII* (Saenger, W., Ed.) Vol. 1b, pp 31–170, Springer-Verlag, Berlin.

Coll, M., Frederick, C. A., Wang, A. H.-J., & Rich, A. (1987) *Proc. Natl. Acad. Sci. U.S.A. 84*, 8385–8389.

Dickerson, R. E., & Drew, H. R. (1981) *J. Mol. Biol. 149*, 761–768.

Dickerson, R. E., Goodsell, D. S., Kopka, M. L., & Pjura, P. E. (1987) *J. Biomol. Struct. Dyn. 5*, 557–579.

DiGabriele, A. D., Sanderson, M. R., & Steitz, T. A. (1989) *Proc. Natl. Acad. Sci. U.S.A. 86*, 1816–1820.

Drew, H. R., McCall, M. J., & Calladine, C. R. (1990) In *DNA Topology and its Biological Effects* (Cozzarelli, N. R., & Wang, J. C., Eds.) pp 1–56, Cold Spring Harbor Laboratory Press, Cold Spring Harbor, NY.

Fitzgerald, P. M. (1988). *J. Appl. Crystallogr. 21*, 273–278.

Fratini, A. V., Kopka, M. L., Drew, H. R., & Dickerson, R. E. (1982) *J. Biol. Chem. 257*, 14686–14707.

Grzeskowiak, K., Yanagi, K., Privé, G. G., & Dickerson, R. E. (1991) *J. Biol. Chem. 266*, 8861–8883.

Hagerman, P. J. (1986) *Nature 321*, 449–450.

Heinemann, U., & Alings, C. (1989) *J. Mol. Biol. 210*, 369–381.

Hendrickson, W. A., & Konnert, J. H. (1980) In *Computing in Crystallography* (Diamond, R., Ramaseshan, S., & Venkatesan, K., Eds.) pp 13.01–13.23, Indian Academy of Sciences, Bangalore.

Klug, A., Jack, A., Viswamitra, M. A., Kennard, O., Shakked, Z., & Steitz, T. A. (1979) *J. Mol. Biol. 131*, 669–680.

Kunkel, G. R., & Martinson, H. A. (1981) *Nucleic Acids Res. 9*, 6869–6888.

Lipanov, A. A., & Chuprina, V. P. (1987) *Nucleic Acids Res. 15*, 5833–5844.

Mahendrasingam, A., Rhodes, H. J., Goodwin, D. C., Nave, C., Pigram, W. J., Fuller, W., Brahms, J., & Vergne, J. (1983) *Nature 301*, 535–537.

Nelson, H. C. M., Finch, J. T., Luisi, B. F., & Klug, A. (1987) *Nature 330*, 221–226.

Prunell, A. (1982) *EMBO J. 1*, 173–179.

Quintana, J. R., Grzeskowiak, K., Yanagi, K., & Dickerson, R. E. (1992) *J. Mol. Biol. 225*, 379–395.

Travers, A. A., & Klug, A. (1987) *Philos. Trans. R. Soc. London B317*, 537–561.

Travers, A. A., & Klug, A. (1990) In *DNA Topology and its Biological Effects* (Cozzarelli, N. R., & Wang, J. C., Eds.) pp 57–106, Cold Spring Harbor Laboratory Press, Cold Spring Harbor, NY.

Ulanovsky, L., Bodner, M., Trifonov, E. N., & Choder, M. (1986) *Proc. Natl. Acad. Sci. U.S.A. 83*, 862–866.

Verdaguer, N., Aymami, J., Fernandez-Forner, D., Fita, I., Coll, M., Huynh-Dinh, T., Igolen, J., & Subirana, J. A. (1991) *J. Mol. Biol. 221*, 623–635.

Vorlickova, M., Sklenar, V., & Kypr, J. (1983) *J. Mol. Biol. 166*, 85–92.

Westhof, E., Dumas, P., & Moras, D. (1985) *J. Mol. Biol. 184*, 119–145.

Wing, R., Drew, H. R., Takano, T., Broka, C., Tanaka, S., Itakura, K., & Dickerson, R. E. (1980 *Nature 287*, 755–758.

Yanagi, K., Privé, G. G. & Dickerson, R. E. (1991) *J. Mol. Biol. 217*, 201–214.

Yoon, C., Privé, G. G., Goodsell, D. S., & Dickerson, R. E. (1988) *Proc. Natl. Acad. Sci. U.S.A. 85*, 6332–6336.

Zinkel, S. S., & Crothers, D. M. (1987) *Nature 328*, 178–181.